LOAD BIAXIALITY EFFECTS ON THE FRACTURE RESISTANCE OF THIN STEEL PLATES

V. P. Naumenko[1] and O. Kolednik[2]

The effect of biaxial loading on the fracture toughness properties of thin steel plates is investigated by testing cruciform centre cracked specimens. The values of the J-integral and the energy dissipation rate are recorded versus the crack extension. Fracture characteristics are determined for initiation of crack growth as well as for the region of steady-state growth. It is shown how these fracture characteristics are influenced by the load biaxiality ratio.

INTRODUCTION

This paper deals with the effect of biaxial loading on the fracture toughness properties of thin steel plates. The experiments are analyzed in terms of traditional and novel energy based fracture characteristics, i.e. in terms of the J-integral and in terms of the energy dissipation rate.

MATERIAL AND EXPERIMENTAL SET-UP

The material tested was a low-carbon sheet steel St.3 (0.14% C, 0.35% Mn, 0.02% Si, 0.01% P, 0.02% S). The tensile testing properties of the material are: yield strength $\sigma_y = 220$ MPa and ultimate tensile strength $\sigma_u = 330$ MPa. The true stress strain curve can be approximated by an equation

$$\frac{\epsilon}{\epsilon_y} = \frac{\sigma}{\sigma_y} + \lambda \left(\frac{\sigma}{\sigma_y} \right)^N , \tag{1}$$

with a strain hardening exponent $N = 4.4$ and a coefficient $\lambda = 16.2$.

From this material cruciform M(T-TC) specimens were machined with a central through crack (see Fig. 1). Additionally, some uniaxial tests were performed on MM(T) specimens (Fig. 1). The thicknesses of the specimens

[1]Institute for Problems of Strength, Academy of Sciences of the Ukraine, 252014 Kiev, Ukraine

[2]Erich-Schmid-Institut für Festkörperphysik, Österreichische Akademie der Wissenschaften, A-8700 Leoben, Austria

were $B = (3.3 \div 3.9)$mm. The data presented in this paper are all for specimens having initial crack lengths of $a_t = 55$ mm.

All specimens were pre-fatigued. Using a special set-up, Pisarenko et al. (1) the specimens were loaded in the longitudinal direction by a tensile or compression load Q which was held constant during the whole test. Subsequently, the tensile load P was applied in the direction transverse to the crack by prescribing the displacement v_P. The magnitudes of the loads, P, Q, the displacements of their application points v_P, v_Q and the vertical displacement v_b at the boundary of the central hole were recorded. On the polished side surface the development of the plastic zone could be observed accurately. From time to time the tip of the blunting and growing crack was photographed. The point of fracture initiation was dedected by observing the midsection region of the blunted crack with an optical microscope.

In performing such tests it is essential to have a uniform stress and strain field in the centre region of the specimen. In former investigations (1) the specimen geometry was optimized by making FEM analyses and photoelastic studies.

TRADITIONAL ANALYSES OF THE TESTS

Fracture initiation and steady-state growth

Independent of the size of the longitudinal load Q, in any case fracture initiation was preceded by the development of narrow plasticity bands on the side surfaces which enveloped completely the specimen ligament. Fracture initiation (indicated as point "i") was defined as the point when the first two or three pores near the midsection of the blunted crack front coalesce. After a transitional stage which is mainly characterized by a fast development of the plastic zone (till it adopts a typical triangular shape) and the formation of a localized neck (see Fig. 2) a steady-state crack extension begins. At the beginning of the steady-state growth (marked with "s") the amount of crack extension is about $\Delta a_s \approx (1 \div 1.5)$ mm. During this steady-state growth the neck moves forward without visually identified changes of its shape or size. At point "j" the steady-state growth is interrupted by a sudden extension of the neck in the horizontal direction through the whole remaining ligament ($h_1 = b = W - a$). (Point "c" marks the beginning of the final unstable fracture.)

Evaluation of J vs. Δa curves

The values of the J-integral were calculated adopting the formulae by Rice et al. (2) and Rakovsky (3), respectively,

$$J = \frac{K^2}{E} + \frac{A^*}{B(W - a_t)} \tag{2}$$

$$J_n^{(\Delta a)} = \frac{W - a_n}{W - a_{n-1}} \left[J_n + J_{n-1}^{(\Delta a)} \right] - J_{n-1}. \tag{3}$$

A^* is a part of the area below the P vs. v_P-record (see Fig. 3). K is determined from the load P and the crack length. $J^{(\Delta a)}$ are corrected J- values allowing for the actual crack length. These values are similar to those following the commonly used ASTM procedure.

For six different longitudinal loads Q the J vs. Δa curves were recorded. Fig. 4 shows the curves for $Q = 0 (k_i = 0)$ and for the largest tensile ($k_i = 1.13$) or compressive $Q (k_i = -1.19)$. k_i denotes the load biaxiality ratio at fracture initiation,

$$k_i = \frac{Q}{P_i}. \tag{4}$$

P_i is the transverse load P at initiation. Only the first 6 mm of crack extension are shown. (Note that the upper curve for $k_i = -1.19$ is correctly drawn because some additional data points follow for larger Δa-vlaues. The data points for $k_i = 0$ can be found in Fig. 5). As expected, the lowest curve is that with the largest (positive) k_i.

Fig. 5 compares the J-Δa-curve of a cruciform M(T-TC) specimen with $k = 0$ to the curve of a MM(T) specimen. In Fig. 6 the dependency of the fracture initiation toughness J_i on the load biaxiality is presented. Additionally, it is shown how the slope of the J-Δa-curves in the steady state region, $(\frac{dJ}{da})_s$, depends on the biaxiality ratio k_s. For evaluating

$$k_s = \frac{Q}{\bar{P}_s} \tag{5}$$

an average of the load P during the steady state region, $\bar{P}_s$, was determined.

Both curves are decreasing with increasing k. The data for the MM(T) specimens are also given: J_i is appeciably higher, $(\frac{dJ}{da})_s$ is much lower than for the M(T- TC) specimens.

Part of these data have been reported already in Pisarenko et al. (4) and in Naumenko and Rakovsky (5). In (5) a dome-shaped J_i vs. k_i curve was presented, ie., the largest J_i was found for $k_i = 0$ and the J_i values decreased for both positive and negative k_i. There are two main reasons for this difference

1. The $J - \Delta a$ curve for $k_i = -2.04$ exhibited a clear "upswing" character due to buckling which in fact invalidates this data. The anti-buckling devices used could not prevent the local buckling near the crack tip at such large negative biaxiality ratios.

2. In (5) it was assumed that M(T-TC) specimens with $k = 0$ and a MM(T) specimen should have nearly identical $J - \Delta a$ curves (see Fig. 5). Further it should be noted that for large biaxiality ratios the $J - \Delta a$ curves seem to be influenced by the size of the initial crack length.

ANALYSES IN TERMS OF THE ENERGY DISSIPATION RATE

Evaluation of D vs. Δa curves

Recently, the energy dissipation rate D has been introduced by Turner (6), as an alternative measure of the crack growth resistance. In Kolednik (7) D was called total crack growth resistance. D is defined as the total amount of non-reversible energy which is necessary to produce an increment of crack extension in a pre-cracked body (7),

$$D \equiv \frac{1}{B}\frac{d}{da}(W_{\mathrm{pl}} + \Gamma) = \frac{1}{B}\frac{d}{da}(U - W_{\mathrm{el}}). \tag{6}$$

U is the work of the applied forces, W_{el} and W_{pl} are the reversible and non-reversible parts of the strain energy, and Γ denotes the surface energy. The right-hand side extension of Eq. (6) follows from an energy balance for stable equilibrium crack extension. D is evaluated experimentally by plotting a $\frac{1}{B}(U - W_{\mathrm{el}})$ vs. Δa-curve which is subsequently differentiated.

Since there are two crack tips in our centre cracked specimens,

$$D \equiv \frac{1}{B}\frac{d}{2da}(W_{\mathrm{pl}} + \Gamma) = \frac{1}{B}\frac{d}{2da}(U - W_{\mathrm{el}}) \tag{7}$$

is the correct form to evaluate the energy dissipation rate from the P vs. v_P records. It is difficult to determine D near to the point of fracture initiation. So we estimated D_i as an average value during the blunting process,

$$D_i = \frac{\Delta(U - W_{\mathrm{el}})_i}{2B\Delta a_i} \approx \frac{\Delta(U - W_{\mathrm{el}})_i}{B\delta_i}. \tag{8}$$

In this rough estimate the relationship $\Delta a_i \approx 0.5\delta_i$ has been adopted, where δ_i denotes the crack tip opening displacement at fracture initiation. In reality the stretched zone width was much smaller than $0.5\,\delta$ but Δa_i also should include the discrete steps of crack extension which occur along the crack front at the point of fracture initiation (see Kolednik and Turner (8), Kolednik and Turner (9)). In Fig. 7 the D vs. Δa curves are drawn. Note that in this diagram the stretched zone width has been neglected and no blunting line is indicated like in the J vs. Δa curves of Fig. 4.

After a small transient regime ($\Delta a \approx 1 \ldots 1.5\,\mathrm{mm}$) during which D decreases rapidly the "steady-state" condition is reached. It should be remarked, however, that even during this "steady-state" growth D_s is decreasing slowly. The lowest curve is that with the largest positive load biaxiality ratio, k.

In Fig. 8 the D_i-values are plotted versus k_i and the $\frac{dD_s}{da}$-values are plotted versus k_s. ($\frac{dD_s}{da}$ gives the slope of the D vs. Δa curves in the region of steady-state growth.) Both curves are decreasing with increasing k. Again, the data for the MM(T) specimens fall out of the trend of the M(T-TC) data.

The relation between resistance curves in terms of D and J

The D vs. Δa curves look like derivatives of the J_R vs. Δa curves. It can be easily shown that this must be so: We consider an increment of steady-state crack extension da after the general yield load P_{GY} has been reached, see Fig. 3. The load line displacement increases by an amount dv_P With Eq. (2) this leads to an increment in J,

$$dJ \approx \frac{dA^*}{bB} = \frac{P_{GY}\, dv_P}{2bB}, \tag{9}$$

because $dW_{\mathrm{el}} \approx 0$ and k remains approximately constant. As dv_P is a plastic displacement ($dv_P^{\mathrm{el}} \approx 0$) the increment in non-reversible strain energy is given by $dW_{\mathrm{pl}} \approx P_{GY}\, dv_P$. With Eq. (7) then follows (when the surface energy Γ is neglected).

$$D \approx \frac{P_{GY}}{2B}\frac{dv_P}{da} \tag{10}$$

Inserting Eq. (9) into Eq. (10) leads to the desired relationship between D and $\frac{dJ}{da}$ for centre cracked panels and fully plastic conditions,

$$D \approx b\frac{dJ}{da}. \tag{11}$$

This derivation is similar to those presented in (7) for bend or deeply notched CT- specimens.

DISCUSSION

Only few reliable data exist on the influence of biaxial loading on the crack growth resistance curves. This is because it is very difficult to make such experiments correctly. E.g., from data not presented here we found that the resistance curves are uncommonly sensitive to changes in initial crack length. The results of Naumenko (10), Naumenko (11) and Naumenko (12) suggest that for high compressive Q-values even the vertical dimension of the pre-crack may have an influence on the test results. The diameter of the central hole must not be too large. A forthcoming paper, Naumenko and Kolednik (13), will be devoted to such topics.

During the analysis of the data presented here we found that we made some mistakes, too, so that this analysis should be considered only as a first approximation to those sought. E.g., we had to exclude some data for higher compressive Q-values because they were invalidated by buckling. The J-Δa-curves showed a typical "upswing" character which can be also found, e.g., in the data presented in Dalle Donne and Döker (14). A more serious because fundamental fault might be that we considered in our analysis only the transverse load and the transverse displacement and neglected the displacement in longitudinal direction v_Q. Some existing data indicate that for high (positive or negative) Q-values the error might be large, but the available data have

not allowed to account for the longitudinal displacement. A similar problem is that it is questionable whether the J-evaluation formula, Eq. (2), is applicable (without making any corrections) for M(T-TC) specimens and biaxial loading.

In recent papers some different proposals have been made how to tackle the effect of in- plane constraint, e.g., Sumpter and Forbes (15), Betegn and Hancock (16), O'Dowd and Shih (17). Most of the data presented are for different geometries but uniaxial loading. It would be interesting to know whether these proposals are good for biaxial loading, too. The authors hope to answer this question in (13).

REFERENCES

(1) Pisarenko, G. S., Naumenko, V. P. and Onishchenko, E. E., Strength of Materials, Vol. 14, 1982, pp. 275–282.

(2) Rice, J. R., Paris, P. S and Merkle, J. G., ASTM STP 536, 1973, pp. 231–245.

(3) Rakovsky, V. A., Strength of Materials, Vol. 14, 1982, pp. 158–163.

(4) Pisarenko, G. S., Naumenko, V. P. and Onishchenko, E. E., Preprint Inst. for Problems of Strength, Ukr. Ac. Sci., Kiev, 1983.

(5) Naumenko, V. P. and Rakovsky, V. A., "Defect Assessment in Components Fundamentals and Applications", Proceedings of ESIS/EGF 9, MEP, London, 1993, pp. 363–377.

(6) Turner, C. E., "Fracture Behaviour and Design of Materials and Structures", Proceedings of ECF8, EMAS, Uk, 1990, Vol. II, pp. 933–968.

(7) Kolednik, O., Engng Fracture Mech., Vol. 38, 1991, pp. 403–412.

(8) Kolednik, O. and Turner, C. E., 25. Vortragsveransttaltung des DVM Arbeitskreises Bruchvorgänge, DVM, 1993, pp. 395–403 (in English).

(9) Kolednik, O. and Turner, C. E., Fat. & Fract. Engng Mats. & Struc., in press.

(10) Naumenko, V. P., Piziko-Khimicheskaya Mekhanika Materialov, Vol. 29, No. 4, 1993 (in Russian).

(11) Naumenko, V. P., Preprint Inst. for Problem of Strength, Ukr. Ac. Sci, Kiev, 1987.

(12) Naumenko, V. P., Soviet Materials Science, March 1992, pp. 484–488.

(13) Naumenko, V. P. and Kolednik, O., to be published.

(14) Dalle Donne, C. and Döker, H., 25. Vortragsveranstaltung des DVM Arbeitskreises Bruchvorgänge, DVM, 1993, pp. 359–369 (in German).

(15) Sumpter, J. D. G. and Forbes, A. T., Proc. of 1st Int. Conf. Shallow Crack Fracture Mechanics, Toughness Tests and Applications, Cambridge, UK, 1992, Paper 7.

(16) Betegn, C. and Hancock, J. W., J. Appl. Mech., Vol. 58, 1991, pp. 104–110.

(17) O'Dowd, N. P. and Shih, C. F., J. Mech. Phys. Solids, Vol. 39, pp. 989–1015.

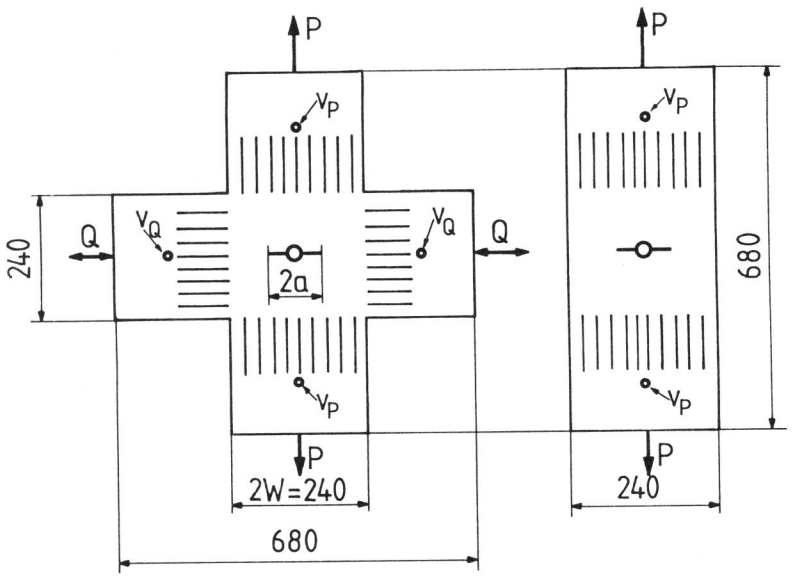

Figure 1: Schematic drawings of cruciform M(T-TC) specimens (left) and MM(T) specimens (right)

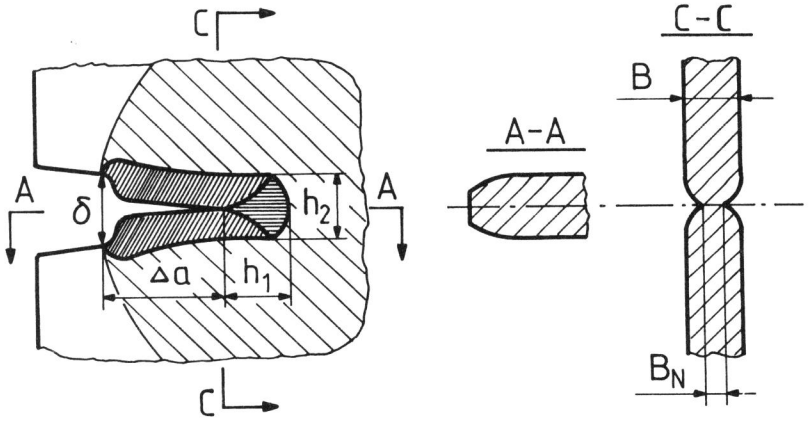

Figure 2: The shape of the localized neck which forms during steady-state growth

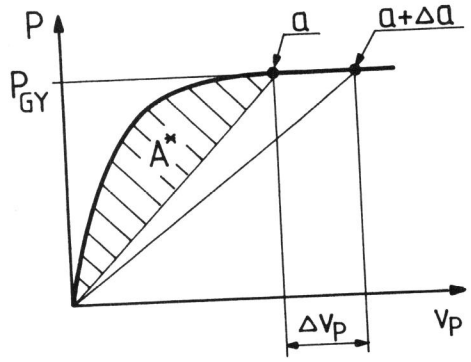

Figure 3: To the J-evaluation formula Eq. (2)

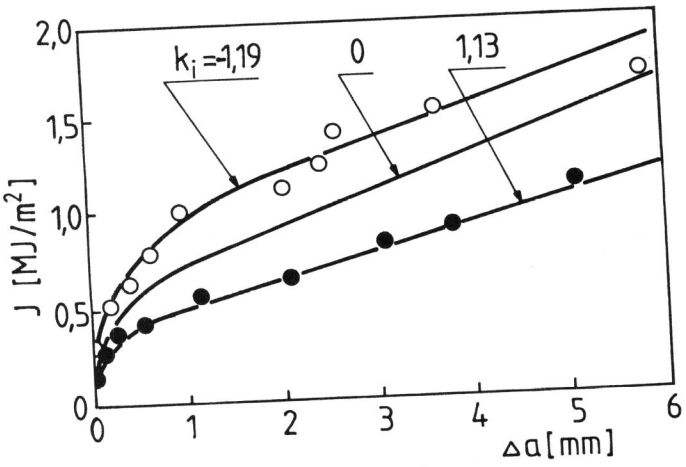

Figure 4: J-integrals vs. crack extension curves for different load biaxiality ratios k_i at initiation

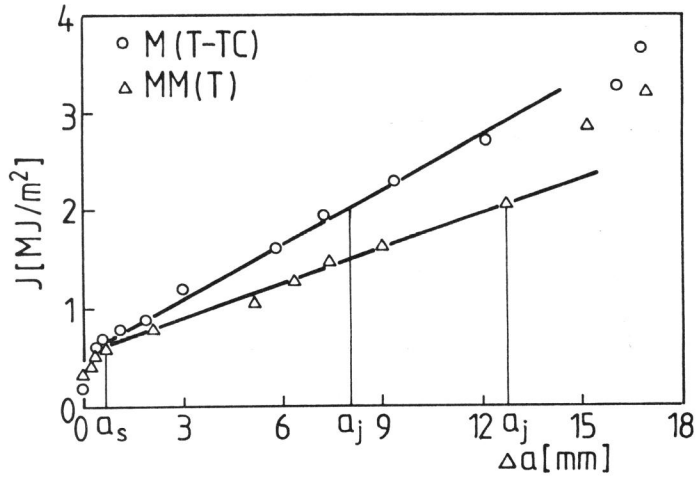

Figure 5: J-integrals vs. crack extension curves for M(T-TC) specimen with $k = 0$ and for $MM(T)$ specimen

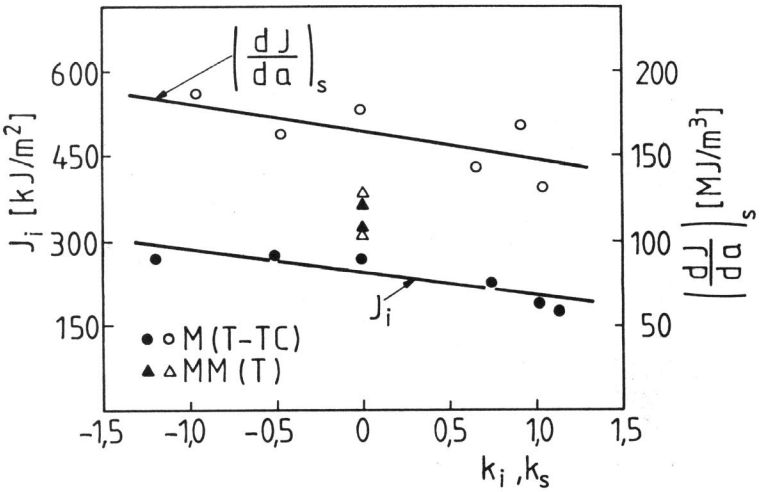

Figure 6: The influence of load biaxiality on J_i (the J-integral at fracture initiation, J_i) and on the slope of the J-Δa-curve in the region of steady-state growth, $(\frac{dJ}{da})_s$

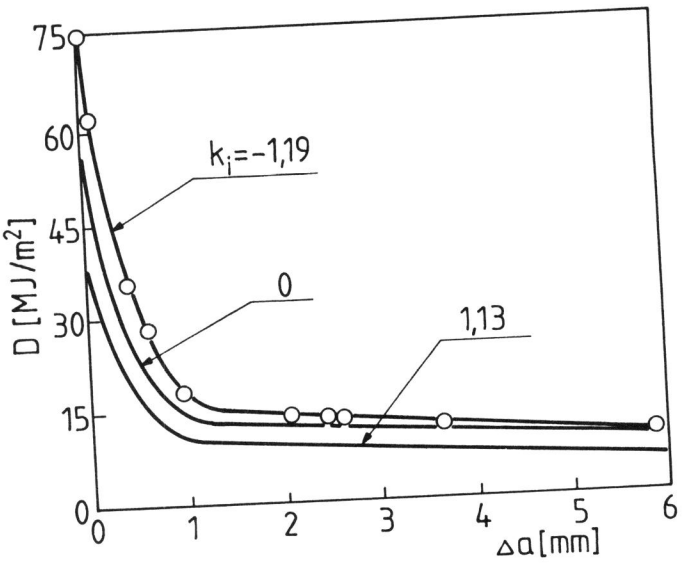

Figure 7: Energy dissipation rate vs. crack extension curves for different load biaxiality ratios k

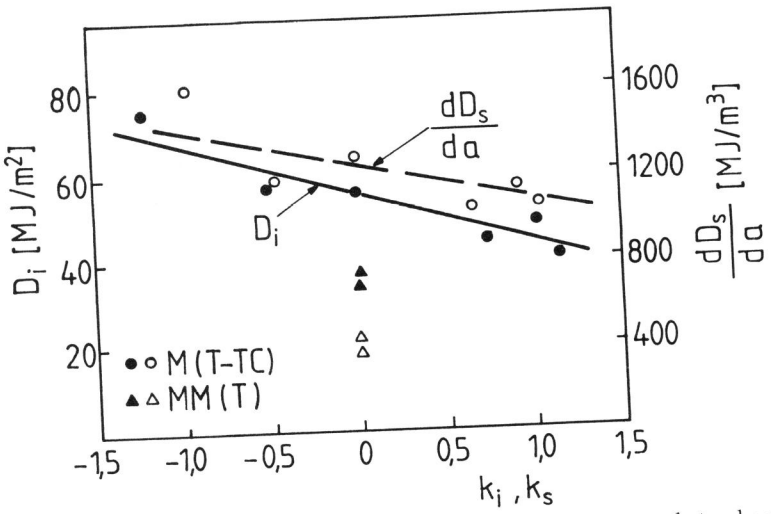

Figure 8: The influence of load biaxiality on fracture initiation and steady-state growth characterized in terms of the energy dissipation rate